RSC Advances

ROYAL SOCIETY
OF CHEMISTRY

www.rsc.org/advances

Graphical Abstract

Generation uniform and small particle size of palladium onto the *SH*-decorated SBA-15 pore-walls: SBA-15/(SH)$_X$Pd-NP$_Y$ as a recoverable nanocatalyst for Suzuki-Miyaura coupling reaction in air and water

Sadegh Rostamnia, Kamran Lamei, Fatemeh Pourhassan

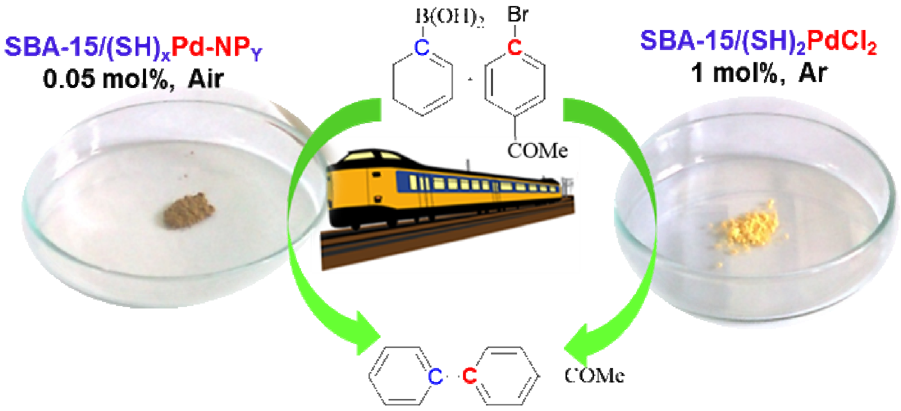

Generation uniform and small particle size of palladium onto the *SH*-decorated SBA-15 pore-walls: SBA-15/$(SH)_X$Pd-NP_Y as a recoverable nanocatalyst for Suzuki-Miyaura coupling reaction in air and water

Sadegh Rostamnia,* Kamran Lamei, Fatemeh Pourhassan

Organic and Nano Group (ONG), Department of Chemistry, Faculty of Science, University of Maragheh, P.O. Box. 55181-83111, Maragheh, Iran: Fax +98(421)2274893; Tel +98(421)2278001(108); E.mail: rostamnia@maragheh.ac.ir; srostamnia@gmail.com

Abstract: Uniform and small particle size of palladium were generated onto the *SH*-decorated SBA-15 pore-walls. The physicochemical properties of the SBA-15/$(SH)_X$Pd-NP_Y were characterized by Fourier transform infrared spectroscopy (FT-IR), X-ray analysis (EDAX), N_2 adsorption/desorption isotherms (BET), scanning electron microscopy (SEM), transmission electron microscopy (TEM) and thermal gravimetric analysis (TGA). The uniform distribution of Pd-NPs into SBA-15 pores was obtained by reduction of SBA-15/$(SH)_2PdCl_2$ using $NaBH_4$ that prepared nanocatalyst was effective catalyst in aerobic Suzuki-Miyaura cross coupling reaction in excellent yields with negligible leaching of Pd-NPs even in water. The SBA-15/$(SH)_X$Pd-NP_Y after easy separation from reaction mixture reused 11 times with high product yields.

Keywords: SBA-15/$(SH)_X$Pd-NP_Y; Suzuki reaction; nanocatalyst; Pd nanoparticle; mesoporous.

1. Introduction

Transition metals (TMs) complexes, clusters and nanoparticles are extremely useful metals on account of their physical or chemical properties [1]. TMs-catalysis makes possible a great many selective and atom-economical transformations. From a green chemistry perspective, immobilization of the TMs are amongst the most important applied catalysis processes [2]. However, existing technologies have their limitations. Palladium as an important transition metal catalysis a broad cross-coupling C-C forming reactions. The Suzuki-Miyaura coupling reaction produce various curative drugs and pharmacological products, that this reaction is often used as a benchmark reaction to estimate the activity of different Pd-based catalysts. [1-4]. Traditionally, the coupling reactions has been performed using homogeneous palladium complexes in the presence of various ligands. These homogeneous catalysts show difficulty in separation of expensive heavy metal catalyst from reaction mixture and suffer from the problems like aggregation of metallic centers and contamination of final reaction products [5]. In addition, the requirement for an inert atmosphere and the use of stoichiometric or relatively expensive reagents, generally unstable and toxic ligands, such as phosphine, are required to activate and stabilize Pd against agglomeration and formation of Pd-black [2,5]. Therefore, Efforts have been focused on immobilization of homogeneous Pd complexes onto different solid supports to facilitate their separation from the products. Various kind of porous support such as mesoporous silica, zeolites, metal-organic frameworks (MOFs), and carbon nanotubes (CNT) have been reported [6]. Because of their properties, SBA-15 ordered mesoporous inorganic materials with uniform pore diameters, large surface areas, tunable structure and modifiable functional groups on surface of channels provide an appropriate scaffold for the immobilization of Pd [7].

In recent years the importance of ligand choice in the success of a catalytic system have studied [8]. Fryxell *et al.* [8a] and Pinnavaia and Mercier [8c] have demonstrated scavenging ability of the *SH*-functionalized mesoporous materials for heavy metal elimination, and Crudden *et al.* [9] have showed the efficiency of Pd encapsulated *SH*-functionalized mesoporous silicates in the Suzuki-Miyaura cross-coupling reaction catalyzes with no leaching of Pd. Herein, we report our work on impregnating palladium nanoparticles (Pd-NPs) into *SH*-functionalized channels of SBA-15 nanoreactor (Scheme 1).

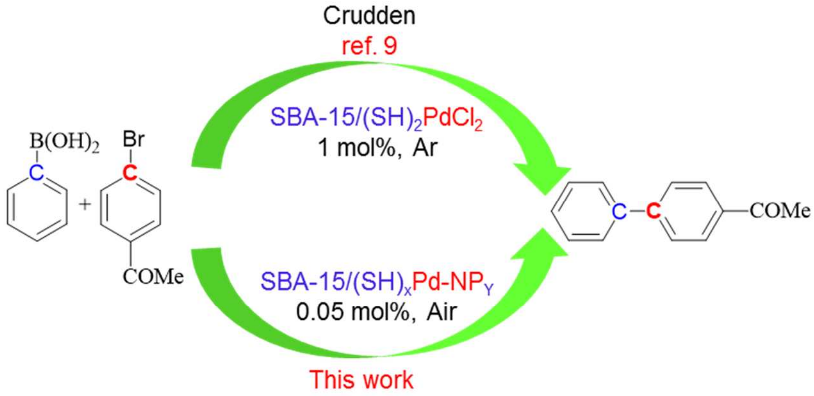

Scheme 1. Studied pathways of Suzuki coupling.

2. Experimental

2.1. Materials and apparatus

Pluronic P123 ($EO_{20}PO_{70}EO_{20}$), tetraethyl orthosilicate (TEOS), potassium carbonate, and other compounds were obtained from Aldrich and were used without further purification. Mercaptopropyl trimethoxysilane (MPTMS) was obtained from Fluka, and was used as received. Solvents were of Certified A.C.S. grade and used as received, though DMF was deoxygenated with bubbling Ar (g) prior to use. X-ray diffraction (XRD) data were collected on a Bruker-D8 Advance X-ray diffractometer with $Cu_{K\alpha}$ radiation with the capillary model, operated at 40 kV and 30 mA. The nitrogen sorption was measured on a Tristar 3000 Micromeritics apparatus. Melting points were measured on an Electrothermal 9100 apparatus. ^1H and ^{13}C NMR spectra were measured ($CDCl_3$) with a Bruker DRX-300 AVANCE spectrometer at 300 and 75 MHz, respectively. The contents of palladium on the prepared solid catalysts and Pd leaching were measured by atomic absorption spectroscopy using residual contents in solvents.

2.2.1. Synthesis of mesoporous silica materials

SBA-15 was synthesized as previously reported [7d, 9]. Typically, 4 g of P123 was dissolved in acidic water (*p*H 2) before the addition of the silica source (9.5 mL TEOS). Condensation of the silica network about the polymer template proceeded for 20 h at 35 ^{o}C before being treated hydrothermally at 100 ^{o}C for 40 h in a sealed vessel. Surfactant was removed from the as-made material by either calcination (1 ^{o}C/min ramp, 600 ^{o}C for 10 h). Propyl thiols were tethered to the silica pore walls by dispersing the as synthesized SBA-15 in dry toluene that contained an excess of MPTMS and refluxing the mixture for 20 h at 100 ^{o}C (see Supporting Information). Sulfur loadings, which was determined by elemental analysis, were 0.7 mmol S/g material. Sufficient $PdCl_2$ or $Pd(OAc)_2$ to afford a 2:1 S:Pd catalyst was then added as a solution in water, then after 1 hour the Cat. A_1 or Cat.A_2 were separated from the solutions. For our main goal, presented Pd (II) ions in mesoporous silica matrix of Cat. A_1, was treated with $NaBH_4$ to produce highly dispersed Palladium nanocatalyst (SBA-15/$(SH)_x$Pd-NP_Y as Cat. A_3). The elemental analysis indicated the ratio of S:Pd is 3.7:1 (for catalyst abbreviations see Fig. 4).

2.2.2. Synthesis of biaryls 3

In a test tube equipped with a magnetic stirrer bar, the aryl halides **1** (1 mmol), was mixed with boronic acid **2** (1.2 mmol), K_2CO_3 (2 mmol), and the Pd-catalyst **(**0.5 mol% Pd) in 3 mL of 1:1 mixture of DMF:H_2O, in air. The reaction mixture was than heated to 80 °C. After completion of the reaction, the reaction was cooled to room temperature, the catalyst was removed by filtration. The catalyst was then washed with Et_2O (3 × 8 mL). The organic layer was separated and dried over anhydrous $MgSO_4$. The solvent was evaporated under reduced pressure to give the corresponding biaryl compounds (see Supporting Information). As a example 4-Methylbiphenyl**:** ^1H NMR: 7.28-7.63 (9 H), 2.44 (3 H). ^{13}C NMR: 141.18, 138.38, 137.03, 129.50, 128.73, 127.23, 127.18, 127.00, 21.11.

2.3. Material characterization

In the FT-IR spectrum of SBA-15 family materials, the band from 799 and ~1100 cm^{-1} is belonged to the vibrations of (Si-O-Si) bond, and the small band at about 960 cm^{-1} is assigned of functionalized (Si-OH) bond and the SiO-H groups are appeared by the very broad IR absorption band in the 3000-3700 cm^{-1} region (Fig. 2). The presence of several bands with low intensity in 1400 and 2900 cm^{-1} region is allocated to SH and its complexes groups. The decrease of the small band in 850-900 and 1600 cm^{-1} band in the spectrum of the SBA-15 indicates the functionalization of the silica surfaces.

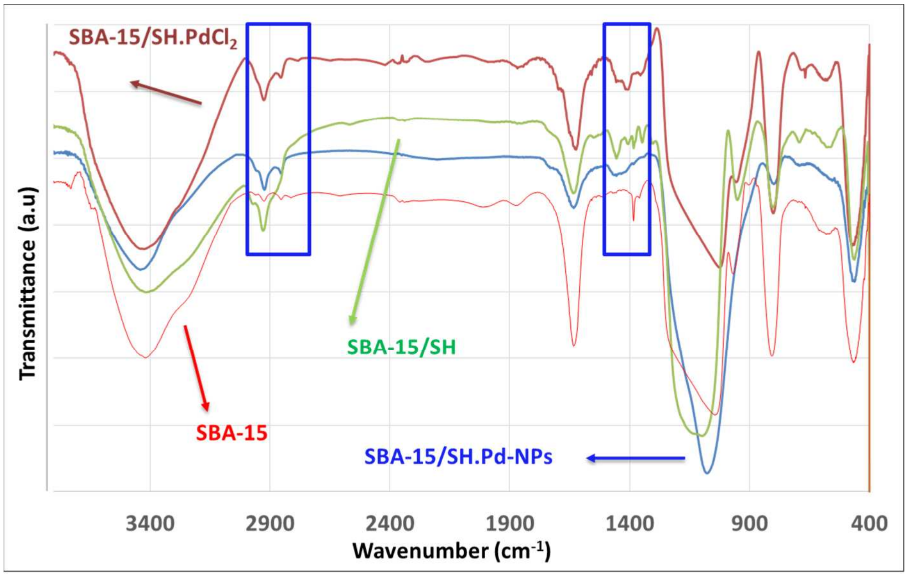

Fig. 1. FTIR spectra of SBA-15 (red), SBA-15/SH (green), SBA-15/SH.$PdCl_2$ (brown) and SBA-15/SH.Pd-NPs (blue)

Fig. 2 shows images of scanning electron microscopy (SEM) and transmission electron microscopy (TEM) of the as synthesized SBA-15 family sample chosen as representative. The highly ordered mesoporous structure of SBA-15 observed by XRD (Fig. 2d), was confirmed by TEM images (Fig. 2c). Diffraction peaks at the below 2° corresponding to the (1 0 0), (1 1 0), and (2 0 0) are readily recognized from the XRD pattern of SBA-15 (Fig 2d). The observed diffraction peaks agree with the 2 D-hexagonal SBA-15 family [8-9].

In fact, Fig. 2c shows the long-chain structure characteristic of the SBA-15 materials as it can be observed by the presence of straight mesochannels arraying along the long axis; meanwhile, the hexagonal arrangement of the unidirectional mesopores is very clear in Fig. 2c where a frontal view of them is presented. It is important to note, that even after the loading of Pd ions and even reduction of the Pd to nanoparticles, the highly ordered structure of the SBA-15 support was retained (Fig. 2e-j). The average mesopore size estimated by TEM is around 7 nm. Transmission electron microscopic (TEM) images of Cat. A_3 showed that Pd nanoparticles were well dispersed inside the nano-channels of functionalized SBA-15 (Fig. 2f). The particle size histogram of SBA-15/$(SH)_x$Pd-NP_Y shows that particle size ranged from 2 nm to 6 nm (Fig. 2h). For this sample, after 11th recycle, segregated Pd-nanoparticles are also observed on the external surface of the silicate and out of pores as it is evidenced by the darker areas in image j in Fig. 2 (Fig. 2j). The particle size histogram of recycled SBA-15/$(SH)_x$Pd-NP_Y and particle size ranged indicated as Fig. 2i.

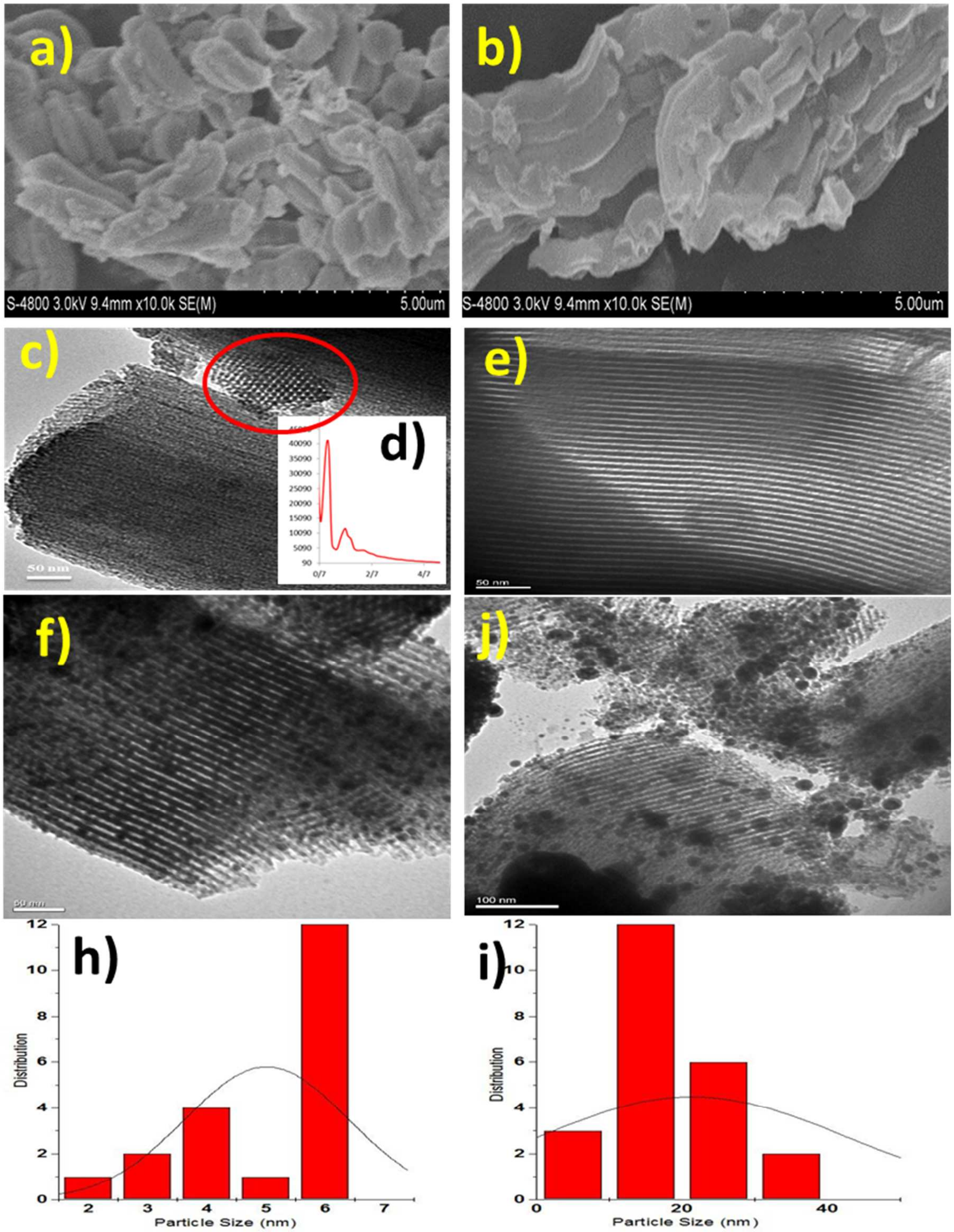

Fig. 2. SEM (a) and TEM (c) images and XRD pattern (d) of SBA-15. TEM (e) images SBA-15/(SH)$_2$PdCl$_2$. SEM (b), TEM (f) images and particle size histogram (h) of SBA-15/(SH)$_X$Pd-NP$_Y$ nanocatalyst. TEM (j) images and particle size histogram (i) of recycled SBA-15/(SH)$_X$Pd-NP$_Y$ nanocatalyst.

To examine the thermal stability of the SBA-15/$(SH)_X$Pd-NP_Y nanocatalyst, thermal gravimetric (TG) were carried out between 30 ^oC and 800 ^oC in a static atmosphere of nitrogen (Fig. 3a). TGA/DTG analysis of SBA-15/$(SH)_X$Pd-NP_Y nanocatalyst shows a weight loss due to the desorption of water below 100 °C followed by a second weight loss centered at 140 °C which is owing to the loss of inner water as well as the loss of CH_3OH upon the further condensation of unreacted methoxy groups. This is finally followed by a set of weight losses centered at 380 °C corresponding to the elimination of the surface bound organic propyl thiol groups (PrSH), which indicates that this nanocatalyst (Cat. A_3) is thermally stable up to 380 °C. For the as synthesized SBA-15 and SBA-15/$(SH)_X$Pd-NP_Y the N_2 physisorption (Fig. 3b) showed the type IV in nature with an H1 hysteresis loop at $p/p_o = 0.6-0.9$ which was typical of mesoporous solids according to the IUPAC classification [10]. The adsorption branch of each isotherm showed a sharp inflection at a relative pressure value of about 0.7, which was particular to capillary condensation within uniform pores [10]. The position of the inflection point was clearly related to a diameter in the mesopore scope. The BET surface area for SBA-15/$(SH)_X$Pd-NP_Y was 341 m^2/g. EDAX was performed to further confirm the composition of the as-prepared products (Fig. 3c). Fig. 3c shows that sample of SBA-15/$(SH)_X$Pd-NP_Y nanocatalyst that is composed of Si, O, and Pd.

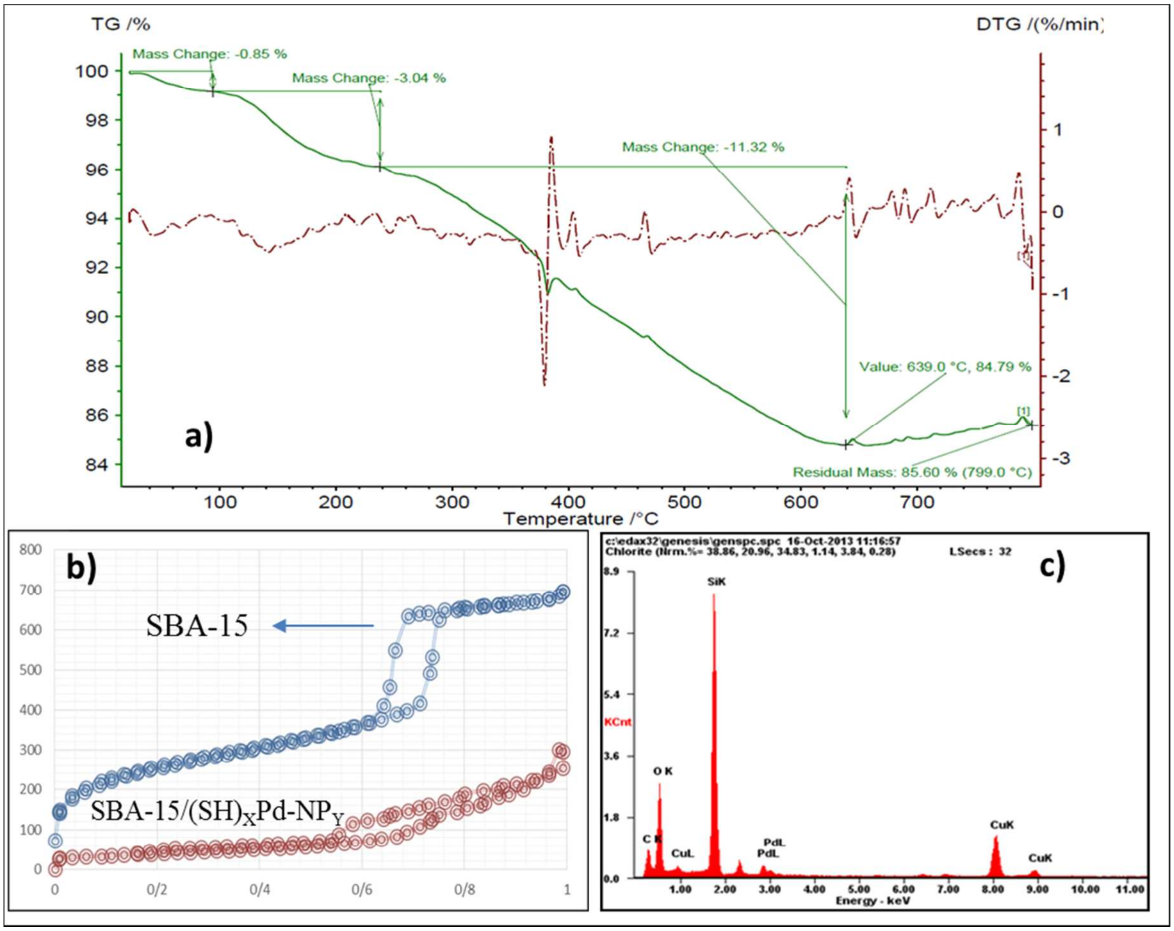

Fig. 3. SBA-15/(SH)$_X$Pd-NP$_Y$ nanocatalyst: TGA/DTG analysis (a), N_2 physisorption isotherms (brown) and EDAX patterns (b) and (c).

3. Results and Discussion

Based on our preliminary works on the synthesis of mesoporous silica materials as catalysts [7,11], mercapto groups (-SH) were first grafted onto the mesoporous silica support. The SBA-15/SH were then loaded with Pd nanoparticles with -SH serving as anchor points. Finally, the SBA-15/(SH)$_X$Pd-NP$_Y$ nanocatalysts were then assessed for the Suzuki-Miyaura C-C cross coupling reaction. In fact, here, we present the results of our study on the efficiency of mercapto-stabilized small sized palladium nanoparticles embedded onto the pore wall of functionalized SBA-15 mesoporous nanoreactor as a highly efficient and green method to the synthesis of biaryls.

The preparation procedure of nanocatalyst (SBA-15/$(SH)_X$Pd-NP_Y) is outlined in Figure 4. The synthesis of catalyst has been achieved in four main steps: in first step we prepared the SBA-15 with known procedure described by Zhao *et al.* [6c] then in second step, thiol functionalization of the SBA-15 occurred by condensation of mercaptopropyl trimethoxysilane with surface silanols. In next two steps, adsorption of the palladium sources [$Pd(OAc)_2$ and $PdCl_2$] with thiol groups and subsequently reduction of immobilized Pd^{II} with MeOH/$NaBH_4$ system lead to the production of high dispersed Pd nanoparticles. The obtained SBA-15/$(SH)_X$Pd-NP_Y nanocatalyst were investigated under both Pd^{II}-anchored pre-catalyst (Cat. A_1 and Cat.A_2) and Pd-NPs pre-catalyst (Cat. A_3 by reduction of Cat. A_1) under Suzuki coupling reaction conditions (Fig. 4).

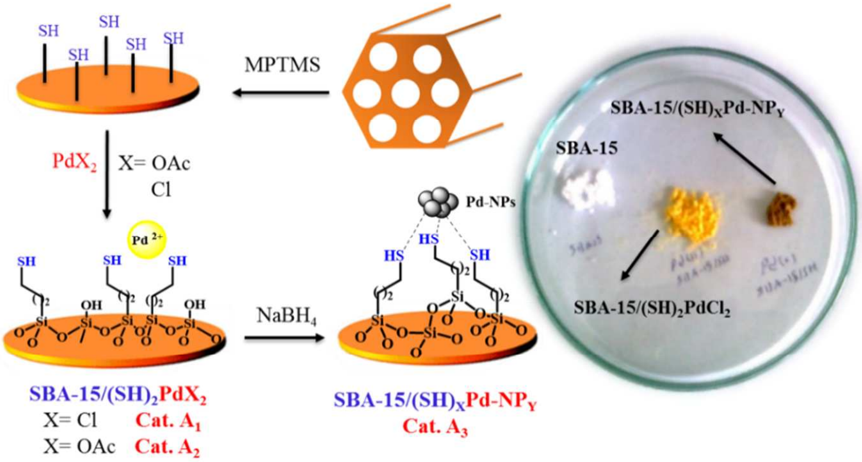

Fig. 4. Schematic representation of catalyst preparation (Cat A_1 - Cat.A_3).

Different types of Pd@SBA-15/SH was investigated under both Pd-anchored pre-catalyst (method I) and directly as ligands (method II) in Suzuki coupling reaction condition (Table 1). For catalytically activity and efficiency purposes, 4-bromoacetophenone, and phenylboronic acid, were chosen as substrates in the coupling model reaction of Suzuki reaction. In the model reaction, to obtain the cross coupled product **3a**, we tested the reaction using catalyst A_1-A_3.

As shown in Table 1, the use of Pd@SBA-15/SH catalysts with different source of Pd (Table 1, catalysts A_1, A_2, A_3) for method II of Cat.A_1 and Cat.A_2 led to the desired product, but in this reactions both the homocoupling product **4** and Pd-black were also detected. Performing the reaction with method I resulted in the production of **3a** in high yields without side products and Pd-black, but the amount of catalysts was 1 mol%. Performing the reaction with Pd-NPs embedded SBA-15/SH just with 0.05 mol% of Pd resulted in the production of **3a** in high yields without any side products. These results shows the high efficiency of the SBA-15/(SH)$_X$Pd-NP$_Y$ catalyst (Cat. A$_3$) in both stability and activity (96% yield of product **3a** with negligible leached Pd).

Table 1. Different catalysts in the model reaction of Suzuki coupling. [a]

Catalyst	Method (I or II)	[Pd]	Mol (%) Pd	S:Pd ratio	(%) Pd-leaching	(%) Yield (**3a**)
Cat. A$_1$	Method I	SBA-15/SH.PdCl$_2$	0.5	2:1	-	98
	Method II	PdCl$_2$ + SBA-15/SH	0.5	2:1	0.61 + Pd-BL[b]	99
Cat. A$_2$	Method I	SBA-15/SH.Pd(OAc)$_2$	0.5	2:1	0.09	94
	Method II	Pd(OAc)$_2$ + SBA-15/SH	0.5	2:1	0.61 + Pd-BL[b]	99
Cat. A$_3$	--	SBA-15/(SH)$_X$Pd-NP$_Y$	0.05	3.7:1	0.05	96

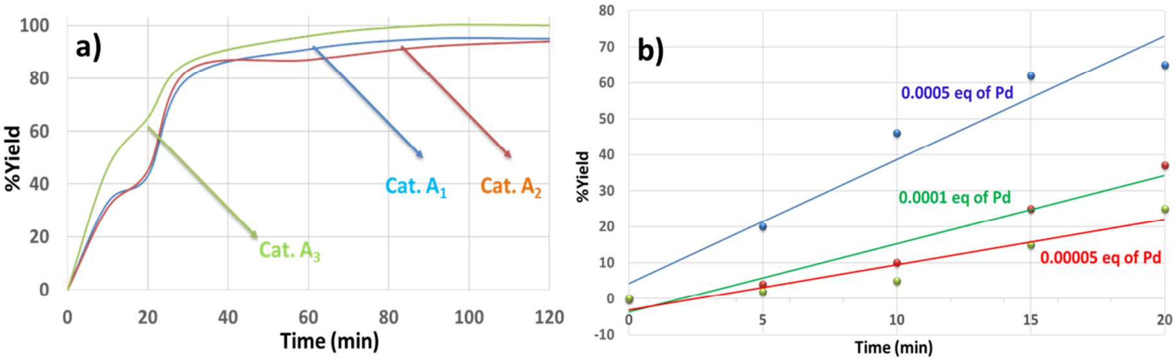

[a] Reaction scale: 1 mmol of substrates. K$_2$CO$_3$ (2 eq.), 80 ^{o}C, 60 min, DMF/H$_2$O (1:1, 4 mL). [b] Pd-black. Reaction progress for the catalysts (a) and different amount of the Pd of SBA-15/(SH)$_X$Pd-NP$_Y$ in reaction condition (b).

For optimization of the reaction conditions, the effect of various parameters such as different solvents, bases, time and Pd mol% in the presence of Cat. A_3 was investigated (model reaction). As shown in Table 2, the best results were obtained using DMF-H_2O (1:1, 2 ml) as the solvent, using K_2CO_3 as base with 0.05 mol% Pd during 0.5 hour (Table 2, entry 7). For comparison, the model reaction was tested under the same conditions but with Cs_2CO_3 as base, the reaction was completed in 25 min with 97% yield of **3a**, without any side products (Table 2, entry 13), but because of availability and price we selected potassium carbonate for next studies.

Table 2. Optimization of model reaction over the Cat.A_3 pre-catalyst. [a]

Entry	Base	Solvent	Mol (%) Pd	Temp (°C)	Time (min)	Yield (%)[b]
1	K_2CO_3	DMF:H_2O[e]	0.06	r.t.	180	trace
2	K_2CO_3	DMF:H_2O[e]	0.06	r.t.	24	40
3	K_2CO_3	DMF:H_2O[e]	0.06	60	60	80
4	K_2CO_3	DMF:H_2O[e]	0.06	80	60	96
5	K_2CO_3	DMF:H_2O[e]	0.05	80	60	97
6	K_2CO_3	DMF:H_2O[e]	0.03	80	60	91
7	K_2CO_3	DMF:H_2O[e]	0.05	80	30	98(100)[c]
8	K_2CO_3	Toluene	0.05	80	20	79
9	K_2CO_3	DMF	0.05	80	20	89
10	K_2CO_3	H_2O	0.05	80	20	84
11	NaOH [d]	DMF:H_2O[e]	0.05	80	60	86
12	Cs_2CO_3	DMF:H_2O[e]	0.05	80	60	96
13	Cs_2CO_3	DMF:H_2O[e]	0.05	80	25	97 (100)[c]
14	K_3PO_4	DMF:H_2O[e]	0.05	80	20	50
15	K_3PO_4	DMF:H_2O[e]	0.05	80	90	60
16	$BaCO_3$	DMF:H_2O[e]	0.05	80	60	10
17	$BaCO_3$	DMF:H_2O[e]	0.05	80	90	20

[a] Reaction conditions: 1 mmol 4-bromoacetophenone, 1.2 mmol phenylboronic acid, 2 mmol base, 3 ml solvent. [b] Isolated yield. [c] Determined by GC. [d] Pd black formed.

Based on discussed results, the catalytic activity of SBA-15/(SH)$_X$Pd-NP$_Y$ in the synthesis of various biaryls by the Suzuki cross-coupling reaction was also studied. Coupling of aryl halide **1** and aryl boronic acid **2** treated under the optimized conditions led to compound **3** (Table 3). Coupling of aryl iodides and boronic acid derivatives gave excellent yields in 20 min. There was no significant difference in the yield of products with Cat. A$_3$ and Cat. A$_1$ (Table 3, entries 2 and 3). Aryl bromides as well as aryl iodides shows high reactivity with boronic acid derivatives in high yields of products in short time (Table 3, entries 4-10).

Table 3. Pd-NPs@SBA-15/SH catalyst Suzuki reactions under optimized conditions. [a]

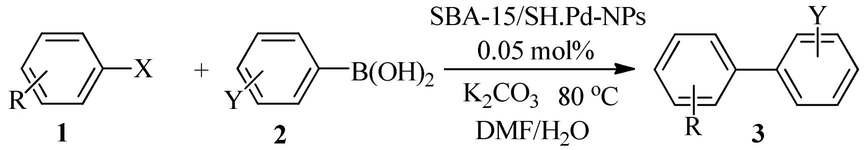

Entry	Ar(R)-	X	Ar(Y)-	Time (min)	**3**	Yield (%)[b]
1	4-MeCOC$_6$H$_4$-	Br	C$_6$H$_5$-	20	**3a**	95
2	C$_6$H$_5$-	I	C$_6$H$_5$-	20	**3b**	97 (100)
3	C$_6$H$_5$-	I	4-MeC$_6$H$_4$-	20	**3c**	97 (100)
4	C$_6$H$_5$-	Br	C$_6$H$_5$-	35	**3d**	97
5	C$_6$H$_5$-	Br	4-MeC$_6$H$_4$-	35	**3e**	95 (98)
6	2-MeC$_6$H$_4$-	Br	C$_6$H$_5$-	35	**3f**	94
7	4-MeC$_6$H$_4$-	Br	C$_6$H$_5$-	35	**3g**	95
8	2-OHCC$_6$H$_4$-	Br	C$_6$H$_5$-	35	**3h**	96
9	3-OHCC$_6$H$_4$-	Br	C$_6$H$_5$-	35	**3i**	95
10	4-MeCOC$_6$H$_4$-	Br	C$_6$H$_5$-	20	**3j**	96
11	C$_6$H$_5$-	Cl	C$_6$H$_5$-	24 h	**3k**	42[c]
12	4-MeCOC$_6$H$_4$-	Cl	C$_6$H$_5$-	24 h	**3l**	46[c]
13	4-MeCOC$_6$H$_4$-	F	C$_6$H$_5$-	24 h	**3m**	Trace

[a] Reaction conditions: 1 mmol aryl halide, 1.2 mmol arylboronic acid, 3 mmol K$_2$CO$_3$, DMF:H$_2$O 3 ml, 80 °C. [b] Isolated yield and in parentheses are GC yield. [c] Containing 0.5 mol% of Pd with 0.5 mmol TBAB.

When the reactions use solid catalysts, the reusability and recovery of the catalysts are important factors. In the model reaction, it was found that supported Pd(0) catalysts has been recovered and reused without considerable loss of theirs reactivity (Fig. 5).

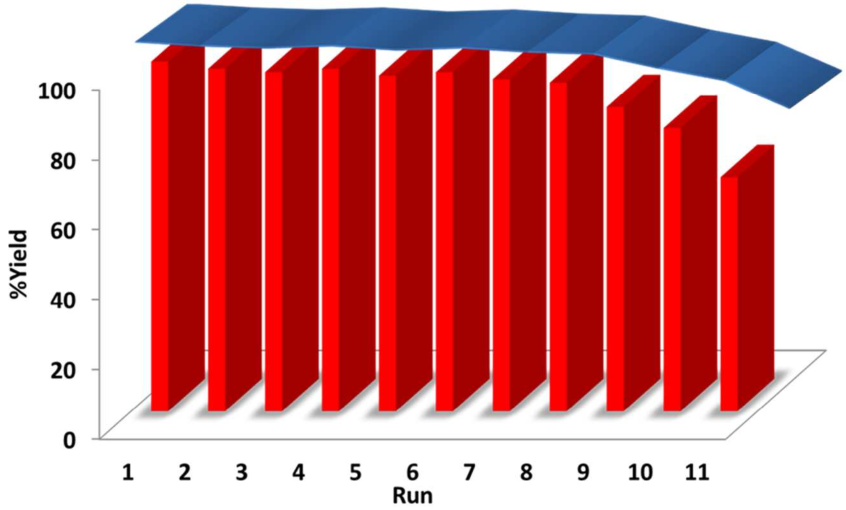

Fig. 5. Recyclability study of SBA-15/(SH)$_X$Pd-NP$_Y$ for model reaction.

4. Conclusions

In summary, highly dispersed Pd-loaded meso-structure nanocatalysts using (3-mercaptopropyl)trimethoxysilane functionalized SBA-15 as support were synthesized. The anchoring thiol groups was effective for the attachment of Pd nanoparticles onto the surface of silica support. In fact, uniform and small particle size of palladium were generated onto the *SH*-decorated SBA-15 pore-walls. This SBA-15/(SH)$_X$Pd-NP$_Y$ efficiently catalyzes Suzuki–Miyaura cross-coupling of aryl halides and boronic acids in excellent yields with negligible leaching of Pd-NPs even in water. The SBA-15/(SH)$_X$Pd-NP$_Y$ after easy separation from reaction mixture reused 11 times with high product yields.

References

1 A. Suzuki, *In Modern Arene Chemistry*, ed. D. Astruc, Wiley-VCH, Weinheim, (2002) Ch. 3, pp. 53-106.

2 L. Yin and J. Liebscher, *Chem. Rev*., 2007, **107**, 133.

3 (a) A. Suzuki, *J. Organomet. Chem*., 1999, **576**, 147; (b) N. Miyaura, A. Suzuki, *Chem. Commun*.,1979, 866-867; (c) N. Miyaura, A. Suzuki, *Chem. Rev*.,1995, **95**, 2457.

4 J.-P. Corbet and G. Mignani, *Chem. Rev*., 2006, **106**, 2651.

5 (a) C. Baleizao, A. Corma, H. Garcia, A. Leyva, *J. Org. Chem*. 2004, **69**, 439; (b) A. Corma, D. Das, H. García, A. Leyva, *J. Catal*. 2005, **229**, 322.

6 (a) B. Karimi and P. Fadavi Akhavan, *Chem. Commun*.,2011, **47**, 7686; (b) S. Rostamnia, H. Xin, *Appl. Organomet. Chem*. 2013, **27**, 348; (c) R. Zhang, W. Ding, B. Tu and D. Zhao, *Chem. Mater*. 2007, **19**, 4379; (d) S. Mandal, D. Roy, R. V. Chaudhari and M. Sastry, *Chem. Mater*. 2004, **16**, 3714; (e) C. D. Wu, A. Hu, L. Zhang and W. B. Lin, *J. Am. Chem. Soc*. 2005, **127**, 8940; (f) X. Pan, Z. Fan, W. Chen, Y. Ding, H. Luo and X. Bao, *Nat. Mater*. 2007, **6**, 507; (g) E. Castillejos, P.-J. Debouttie` re, L. Roiban, A. Solhy, V. Martinez, Y. Kihn, O. Ersen, K. Philippot, B. Chaudret and P. Serp, *Angew. Chem., Int. Ed*. 2009, **48**, 2529.

7 (a) A. Corma, *Chem. Rev*. 1997, **97**, 2373; (b) A. Corma, H. Garcia, *Adv. Synth. Catal*. 2006, **348**, 1391; (c) C. T. Kresge, M. E. Leonowicz, W. J. Roth, J. C. Vartuli and J. S. Beck, *Nature*, 1992, **359**, 710; (d) D. Zhao, J. Feng, Q. Huo, N. Melosh, G. H. Fredrickson, B. F. Chmelka and G. D. Stucky, *Science* 1998, **279**, 548; (e) S. Rostamnia, H. Xin, X. Liu, K. Lamei, *J. Mol. Catal. A: Chemical*, 2013, **374-375**, 85; (f) Rostamnia, F. Pourhassan, *Chin. Chem. Lett*., 2013, **24**, 401.

8 (a) T. E. Barder, S. D. Walker, J. R. Martinelli, S. L. Buchwald, *J. Am. Chem. Soc*. 2005, **127**, 4685; (b) X. Feng, G. E. Fryxell, L. Q. Wang, A. Y. Kim, J. Liu,K. M. Kemner. *Science* 1997, **276**, 923; (c) L. Mercier, T. J. Pinnavaia, *Adv. Mater*. 1997, **9**, 500.

9 (a) C. M. Crudden, M. Sateesh, R. Lewis, *J. Am. Chem. Soc*. 2005, **127**, 10045; (b) Ben W. Glasspoole, Jonathan D. Webb, Cathleen M. Crudden. *J. Catal*. 2009, **265**, 148; (c) C.M. Crudden, K. McEleney, S.L. MacQuarrie, A. Blanc, M. Sateesh, J.D. Webb, *Pure Appl. Chem*. 2007, **79**, 247.

10 (a) K.S.W. Sing, D.H. Everett, R.A.W. Haul, L. Moscow, R.A. Pierotti, J. Rouquerol, T. Siemieniewska, *Pure Appl. Chem*. 1985, **57**, 603; (b) S.J. Gregg, K.S.W. Sing, Adsorption, Surface Area and Porosity, 2nd ed., Academic Press, London, 1982.

11 (a) S. Rostamnia, K. Lamei, *Synthesis* 2011, 3080; (b) S. Rostamnia, K. Lamei, M. Mohammadquli, M. Sheykhan, A. Heydari, *Tetrahedron Lett*. 2012, **53**, 5257; (c) S. Rostamnia, A. Zabardasti, *J. Fluorine Chem*. 2012, **144**, 69; (d) S. Rostamnia, A. Hassankhani, H. G. Hossieni, B. Gholipour, H. Xin, *J. Mol. Catal. A: Chem.* 2014, **395**, 463; (e) S. Rostamnia, X. Liu, D. Zheng, *J. Colloid. Interface. Sci.*, 2014, **432**, 86; S. Rostamnia, E. Doustkhah, *RSC Adv.*, 2014, **4**, 28238; (f) S. Rostamnia, Z. Karimi, M. Ghavidel, *J. Sulf. Chem*., 2012, **33**, 313.